Microbiology (2016), **162**, 1922–1932 **DOI** 10.1099/mic.0.000371

Specific *Bacillus subtilis* 168 variants form biofilms on nutrient-rich medium

Ramses Gallegos-Monterrosa,† Eisha Mhatre† and Ákos T. Kovács

Terrestrial Biofilms Group, Institute of Microbiology, Friedrich Schiller University Jena, Jena, Germany

Correspondence
Ákos T. Kovács
akos-tibor.kovacs@uni-jena.de

Received 5 August 2016
Accepted 9 September 2016

Bacillus subtilis is an intensively studied Gram-positive bacterium that has become one of the models for biofilm development. *B. subtilis* 168 is a well-known domesticated strain that has been suggested to be deficient in robust biofilm formation. Moreover, the diversity of available *B. subtilis* laboratory strains and their derivatives have made it difficult to compare independent studies related to biofilm formation. Here, we analysed numerous 168 stocks from multiple laboratories for their ability to develop biofilms in different set-ups and media. We report a wide variation among the biofilm-forming capabilities of diverse stocks of *B. subtilis* 168, both in architecturally complex colonies and liquid–air interface pellicles, as well as during plant root colonization. Some 168 variants are indeed unable to develop robust biofilm structures, while others do so as efficiently as the non-domesticated NCIB 3610 strain. In all cases studied, the addition of glucose to the medium dramatically improved biofilm development of the laboratory strains. Furthermore, the expression of biofilm matrix component operons, *epsA-O* and *tapA-sipW-tasA*, was monitored during colony biofilm formation. We found a lack of direct correlation between the expression of these genes and the complexity of wrinkles in colony biofilms. However, the presence of a single mutation in the exopolysaccharide-related gene *epsC* correlates with the ability of the stocks tested to form architecturally complex colonies and pellicles, and to colonize plant roots.

INTRODUCTION

Bacillus subtilis is a non-pathogenic model Gram-positive bacterium that has been extensively studied for over a century. Microbiologists have used *B. subtilis* to investigate a broad variety of biological questions, ranging from the intricacies of cell metabolism to community behaviour and evolution (Earl *et al.*, 2008; Shank & Kolter, 2011). As a consequence of the extended use of *B. subtilis*, multiple strains exist in laboratories and strain collections all over the globe. Some of these strains have been isolated from distinct environments and are used as wild-type reference strains, e.g. NCIB 3610 (from here onwards, 3610) and PS216. Other commonly used strains have been described as 'domesticated' due to their prolonged use under laboratory conditions, which have conferred them with characteristics that make them ideal research models, i.e. ease of genetic manipulation and efficient growth on commercially available media.

One of the key features of *B. subtilis* is its ability to form biofilms. Biofilms are complex multicellular communities that can develop in diverse environments and potentially have a major impact on multiple human activities, among others including an ominous progression of common infections or hampering of biotechnological and industrial applications (Bjarnsholt *et al.*, 2013; Valderrama & Cutter, 2013). Formation of biofilms can be desirable under certain circumstances; *B. subtilis* biofilms, for example, have been implicated in crop protection by prevention of colonization of plant roots by pathogenic organisms (Bais *et al.*, 2004).

B. subtilis has become one of the model organisms used for biofilm research. Studies performed over the years have provided many insights regarding the processes involved in the development of these bacterial populations (Mhatre *et al.*, 2014; Mielich-Süss & Lopez, 2015). Strain 168 is the most well-known and widely used laboratory strain; it is an easily transformable tryptophan auxotroph that was obtained by X-ray mutagenesis (Burkholder & Giles, 1947) and has been used in a multitude of academic and industrial studies. The intensive use of strain 168 has generated various derivative strains, several of which have been sequenced by a joint European–Japanese consortium and later re-sequenced using single strains (Barbe *et al.*, 2009; Kunst *et al.*, 1997; Zeigler *et al.*, 2008).

†These authors contributed equally to this work.

Abbreviation: ROI, region of interest.

Three supplementary figures are available with the online Supplementary Material.

The biofilms formed by *B. subtilis* have traditionally been studied as complex structured colonies on agar plates or as pellicles formed at the liquid–air interface of static liquid cultures (Cairns *et al.*, 2014; Vlamakis *et al.*, 2013). Branda *et al.* (2001) were the first to report the various biofilms developed by certain *B. subtilis* strains, noticing that domesticated laboratory strains derived from strain PY79 formed deficient biofilms. Since then, laboratory strains, including 168, have largely been considered as poor or non-biofilm formers at best (Romero, 2013). Different studies have investigated the genetic differences between this strain and wild-type 3610, reporting that these disparities are responsible for strain 168's small, unstructured colonies and flat, featureless pellicles (McLoon *et al.*, 2011; Pollak *et al.*, 2015). In particular, a deficiency in the production of exopolysaccharide (EPS) has been highlighted as an important flaw of strain 168 related to biofilm formation (Kearns *et al.*, 2005; McLoon *et al.*, 2011).

In *B. subtilis*, EPS is produced by the proteins encoded in the *epsA-O* operon (Branda *et al.*, 2004) and is a major component of the biofilm matrix (Flemming & Wingender, 2010). Due to its relevance to biofilm formation, the chemical nature of this polymer has been investigated by various groups. However, these studies have normally used different non-domesticated strains and media, obtaining disparate results (Chai *et al.*, 2012; Jones *et al.*, 2014; Roux *et al.*, 2015). This phenomenon is a testament to the robustness of *B. subtilis*, a soil bacterium that has evolved the ability to survive on different nutrient sources and therefore can use diverse compounds to produce the polymers that form the backbone of the biofilm matrix (Kohlstedt *et al.*, 2014; Meyer *et al.*, 2014).

A problem that permeates *B. subtilis* research is the plethora of available strains and methods, making it difficult to compare experimental results. Here, we compared various biofilms developed by divergent laboratory stocks of strain 168 originating from various research groups around the globe. We also analysed the expression of the *eps* and *tapA-sipW-tasA* operons using fluorescent reporter fusion. We report that the formation of complex colonies varies greatly among the various 168 strains, some of them being able to form architecturally complex colonies similar to those developed by 3610 when grown on complex or supplemented media. In addition, we show that the expressions of P_{eps}-GFP and P_{tapA}-GFP fusion does not necessarily correlate with the formation of architecturally complex structures in these biofilms.

METHODS

Strains and media. All strains used in this study are listed in Table 1. These strains were pre-grown overnight in LB medium (lysogeny broth, Carl Roth; 10 g l^{-1} tryptone, 5 g l^{-1} yeast extract and 5 g l^{-1} NaCl) and later grown on LB supplemented with 0.1 mM $MnCl_2$ and either 0.1 % glucose (hereafter, LB-Glu) or 1 % glycerol (hereafter, LB-Gly), 2×SG medium [16 g l^{-1} nutrient broth (Difco), 2 g l^{-1} KCl, 0.5 g l^{-1} $MgSO_4 \cdot 7H_2O$, 1 mM $Ca(NO_3)_2$, 0.1 mM $MnCl_2 \cdot 4H_2O$, 1 μM $FeSO_4$ and 0.1 % glucose] (Kobayashi, 2007) or defined MSgg medium [5 mM potassium phosphate buffer (pH 7), 100 mM MOPS, 2 mM $MgCl_2$, 700 μM $CaCl_2$, 100 μM $MnCl_2$, 50 μM $FeCl_3$, 1 μM $ZnCl_2$, 2 μM thiamine, 0.5 % glycerol, 0.5 % glutamate, 50 μM L-tryptophan and 50 μM L-phenylalanine] adapted from Branda *et al.* (2001). Murashige and Skoog (MS) medium was used for *Arabidopsis thaliana* germination [MS basal salt mixture, Sigma-Aldrich; 2.2 g l^{-1} MS medium (pH 5.6–5.8)], while MSNg medium was used for root surface colonization assays [5 mM potassium phosphate buffer (pH 7), 100 mM MOPS, 2 mM $MgCl_2$, 50 μM $MnCl_2$, 1 μM $ZnCl_2$, 2 μM thiamine, 0.2 % NH_4Cl, 0.05 % glycerol and 700 μM $CaCl_2$]. Media were supplemented with Bacto agar 1.5 or 1 % when solid plates were needed for bacterial colonies or plant seed germination, respectively. Unless otherwise stated, all liquid cultures were grown at 37 °C with shaking at 225 r.p.m.

Strain construction. *B. subtilis* P_{eps}-GFP and P_{tapA}-GFP strains were obtained via natural competence transformation (Kunst & Rapoport, 1995) using genomic DNA from strains NRS2243 and NRS2394, respectively. Briefly, overnight cultures of the receiver strains were diluted to a 1 : 50 ratio with GCHE medium [1 % glucose, 0.2 % glutamate, 100 mM potassium phosphate buffer (pH 7), 3 mM trisodium citrate, 3 mM $MgSO_4$, 22 mg l^{-1} ferric ammonium citrate, 50 mg l^{-1} L-tryptophan and 0.1 % casein hydrolysate], and these cultures were incubated for 4 h, after which 5–10 μg of genomic DNA was mixed with 500 μl of competent cells and further incubated for 2 h before plating. $P_{hyperspank}$-GFP labelled strains were obtained by the same method using plasmid phyGFP that integrates into the *amyE* locus of *B. subtilis* (van Gestel *et al.*, 2014). Transformants were selected on LB plates with 5 μg ml^{-1} kanamycin or 5 μg ml^{-1} chloramphenicol. In all transformations, several clones were examined for colony morphology and no phenotypical differences regarding wrinkleability were observed between the obtained transformants and their corresponding parental strains. Successful transformation was validated using the fluorescence reporter activity of the strains or amylase-negative phenotype on 1 % starch agar plates (Harwood & Cutting, 1990). DK1042 was used rather than 3610 to obtain fluorescently labelled strains, due to its improved transformability (Konkol *et al.*, 2013).

Biofilm development as pellicles and architecturally complex colonies. The study strains were pre-grown in 3 ml LB medium overnight, following which 2 ml of 1 : 50 dilution of these cultures in 2×SG and MSgg media were used to inoculate 24-well plates for pellicle formation. For biofilm colony structures, the four types of media (LB-Glu, LB-Gly, 2×SG and MSgg) were supplemented with 1.5 % agar and tempered to 55 °C, and 25 ml of the medium was poured into a 90 mm-diameter Petri dish. Once solid, plates were dried completely open in a laminar airflow bench for exactly 15 min. The plates were closed and 2 μl of each strain was inoculated on to the plate. To avoid growth inhibition and constraint resulting from two different *B. subtilis* strains, only three strains were inoculated per plate and each had the reference 168 Je strain for comparison of morphology. The plates for the pellicles and colonies were incubated at 30 °C for 72 h.

Biofilm development on root surfaces. Seeds of *A. thaliana* ecotype Col-0 were surface sterilized by incubation in 1 ml of 2 % NaClO solution for 20 min on an orbital mixer. The seeds were washed five times with 1 ml of sterile distilled water and placed on MS medium supplemented with 1 % agar (Oslizlo *et al.*, 2015). The seeds were planted 15 mm apart in order to avoid entanglement of the roots. The MS plates were parafilm sealed and incubated at 4 °C for 72 h, following which they were placed at room temperature on a windowsill for 10–12 days to allow the seeds to germinate and develop roots of approximately 1 cm in length. Overnight cultures of the test strains were adjusted to OD_{600} of 0.2 and then further diluted 10-fold using MSNg medium. The seedlings were then placed in 300 μl of these cultures in a 48-well microplate. The roots of the seedlings were completely submerged in the bacterial dilutions. The microplate was incubated at 28 °C with 90 r.p.m. shaking for

Table 1. Strains used in this study

Strain	Characteristics	Abbreviation used here	Reference
3610	Prototroph, wild-type	3610	Bacillus Genetic Stock Center (BGSC)
DK1042	3610 *comI*^{Q12I}		Konkol *et al.* (2013)
NRS2243	3610 *sacA* ::P$_{epsA}$-*gfp* (*neo*), *hag*::*cat*		Murray *et al.* (2009)
NRS2394	3610 *sacA*::P$_{tapA}$-*gfp* (*neo*)		Murray *et al.* (2009)
JH642	Δ*trpC2* Δ*pheA1 citS642*, derived from Marburg strain		Laboratory Stock (Grau, R., originally from Hoch, J.A.)
168 (Boston)	Δ*trpC2*, derived from 168	168 Bo	Laboratory Stock (Romero, D., originally from Kolter, R.)
168 (Braunschweig)	Δ*trpC2*, derived from 168	168 Br	Laboratory Stock (Härtig, E.)
168 (Göttingen)	Δ*trpC2*, derived from 168	168 Gö	Laboratory Stock (Stülke, J.)
168 (Jena)	Δ*trpC2*, derived from 168 1A700	168 Je	Laboratory Stock (Terrestrial Biofilms Group, originally from University of Groningen and BGSC)
168 (Ljubljana)	Δ*trpC2*, derived from 168 1A1	168 Lj	Laboratory Stock (Mandić-Mulec, I., originally from BGSC)
168 (Malaga)	Δ*trpC2*, derived from 168	168 Ma	Laboratory Stock (Romero, D.)
168 (Münich)	Δ*trpC2*, derived from 168	168 Mü	Laboratory Stock (Thorsten, M., originally from Stülke, J.)
168 (New Castle)	Δ*trpC2*, derived from 168 1A1	168 NC	Laboratory Stock (Veening, J.-W. and Errington, J., originally from BGSC)
168 (Paris)	trp+, tryptophan-prototrophic derivative of 168 (with reconstituted *trpC* gene)	168 Pa	Laboratory Stock (Briandet, R., BaSysBio reference strain, BSB1) (Nicolas *et al.*, 2012)
168 (Pavia 1)	Δ*trpC2*, derived from 168	168 P1	Laboratory Stock (Calvio, C., originally from Anagnostopoulos)
168 (Pavia 2)	Δ*trpC2*, derived from 168	168 P2	Laboratory Stock (Calvio, C., originally from Burkholder and Giles)
168 (Tokai)	Δ*trpC2*, derived from 168	168 To	Laboratory Stock (Ogura, M., originally from the EU sequencing consortium)
TB356	168 NC *sacA*::P$_{epsA}$-*gfp* (*neo*)		This study
TB357	168 Gö *sacA*::P$_{epsA}$-*gfp* (*neo*)		This study
TB358	168 To *sacA*::P$_{epsA}$-*gfp* (*neo*)		This study
TB359	168 Br *sacA*::P$_{epsA}$-*gfp* (*neo*)		This study
TB360	168 P1 *sacA*::P$_{epsA}$-*gfp* (*neo*)		This study
TB361	168 P2 *sacA*::P$_{epsA}$-*gfp* (*neo*)		This study
TB362	JH642 *sacA*::P$_{epsA}$-*gfp* (*neo*)		This study
TB363	DK1042 *sacA*::P$_{epsA}$-*gfp* (*neo*)		This study
TB365	168 Je *sacA*::P$_{epsA}$-*gfp* (*neo*)		This study
TB392	168 Bo *sacA*::P$_{epsA}$-*gfp* (*neo*)		This study
TB394	168 Ma *sacA*::P$_{epsA}$-*gfp* (*neo*)		This study
TB366	168 NC *sacA*::P$_{tapA}$-*gfp* (*neo*)		This study
TB367	168 Gö *sacA*::P$_{tapA}$-*gfp* (*neo*)		This study
TB368	168 To *sacA*::P$_{tapA}$-*gfp* (*neo*)		This study
TB369	168 Br *sacA*::P$_{tapA}$-*gfp* (*neo*)		This study
TB370	168 P1 *sacA*::P$_{tapA}$-*gfp* (*neo*)		This study
TB371	168 P2 *sacA*::P$_{tapA}$-*gfp* (*neo*)		This study
TB372	JH642 *sacA*::P$_{tapA}$-*gfp* (*neo*)		This study
TB373	DK1042 *sacA*::P$_{tapA}$-*gfp* (*neo*)		This study
TB375	168 Je *sacA*::P$_{tapA}$-*gfp* (*neo*)		This study
TB393	168 Bo *sacA*::P$_{tapA}$-*gfp* (*neo*)		This study
TB395	168 Ma *sacA*::P$_{tapA}$-*gfp* (*neo*)		This study
TB34	DK1042 *amyE*::P$_{hyperspank}$-*gfp* (*cat*)		Seccareccia *et al.* (2016)
TB49	168 Je *amyE*::P$_{hyperspank}$-*gfp* (*cat*)		van Gestel *et al.* (2014)
TB707	168 Bo *amyE*::P$_{hyperspank}$-*gfp* (*cat*)		This study

Table 1. cont.

Strain	Characteristics	Abbreviation used here	Reference
TB709	168 P1 *amyE*::$P_{hyperspank}$-*gfp* (*cat*)		This study
TB722	168 Gö *amyE*::$P_{hyperspank}$-*gfp* (*cat*)		This study
TB723	168 Lj *amyE*::$P_{hyperspank}$-*gfp* (*cat*)		This study

24 h. After the incubation period, the seedling roots were gently washed three times with sterile MSNg medium, placed on microscopy slides, covered with coverslips and examined without further treatment.

Microscopy and image analysis. All bright-field and green fluorescence images of colonies and pellicles were obtained with an Axio Zoom V16 stereomicroscope (Carl Zeiss) equipped with a Zeiss CL 9000 LED light source, HE eGFP filter set (excitation at 470/40 nm and emission at 525/50 nm) and an AxioCam MRm monochrome camera (Carl Zeiss). For colony and pellicle morphology comparison, images were obtained after 72 h incubation at ×5 and ×20 magnifications. For P_{eps}-GFP and P_{tapA}-GFP reporter fusion expression comparison, images were taken at different time points using ×3.5 magnification and exposure times of 2500 ms for green fluorescence and 10 ms for bright field.

The expression of green fluorescence of colonies was analysed using ImageJ (National Institutes of Health). Briefly, images were batch processed to subtract a background value, and this value was calculated using a circular region of interest (ROI) of 1 mm radius and measuring the average fluorescence intensity in 36 non-colony areas selected from random images at all time points using only the green channel information. Afterwards, the colony area of each image was selected using the bright-field channel and the tracing tool with legacy mode and a tolerance of 100. Using the selected ROI, the corresponding colony areas were marked on the green fluorescence images and their average fluorescence intensity was measured.

All bright-field and green fluorescence images of *A. thaliana* roots were obtained with an Axio Observer 780 Laser Scanning Confocal Microscope (Carl Zeiss) equipped with a Plan-Apochromat 63×/1.4 Oil DIC M27 objective, an argon laser for stimulation of green fluorescence (excitation at 488 nm and emission at 540/40 nm), a halogen HAL-100 lamp for transmitted light microscopy and an AxioCam MRc colour camera (Carl Zeiss). The images were obtained as a Z-stack of 10 slices covering 3.8 µm on the Z-axis. The images were later merged with ImageJ using an average-intensity Z-projection. The average fluorescence intensity of the roots was measured by selecting the root area as an ROI in the bright-field channel and then measuring the fluorescence intensity in the corresponding area of green channel Z-projections only.

Sequencing of *epsC*, *swrA*, *degQ* and *sfp* alleles. Fragments of *epsC* (788 bp), *swrA* (935 bp), *degQ* (552 bp) and *sfp* (827 bp) were PCR amplified from genomic DNA of the tested *B. subtilis* stocks using corresponding primer pairs (Table 2). The fragments were sequenced using primer oTB110 (*epsC*), oTB131 (*swrA*), oTB132 (*degQ*) or oTB134 (*sfp*) (GATC Biotech).

RESULTS

Various stocks of *B. subtilis* 168 show diverse complex colony and pellicle morphologies

Different nutrients are known to have a profound effect on general metabolism and the production of signalling molecules that regulate biofilm formation in *B. subtilis* (Mhatre *et al.*, 2014). Previous publications suggest that the availability of complex nutrients might supplement the metabolic shortcomings of strain 168 and allow it to develop architecturally complex biofilms (Kovács & Kuipers, 2011; Mhatre *et al.*, 2016). We were interested in testing various stocks of the 168 strain that are used by different laboratories. Importantly, these stocks might have diverged due to additional genetic differences, possibly resulting in contrasting observations among the work groups investigating biofilm formation.

We grew complex colonies of the 168 variants obtained, the domesticated laboratory strain JH642 and the wild isolate 3610 on defined (i.e. MSgg) and complex (i.e. supplemented LB and 2×SG) media for 72 h. LB, although rich in nutrients and commonly used by microbiologists, is not a biofilm-promoting medium. The colonies developed by *B. subtilis* on LB agar are small, flat and featureless, and no pellicles develop on static liquid LB cultures (data not shown). We investigated the possibility that the addition of both manganese and carbon sources (glycerol or glucose) similar to those present in other media could be sufficient to promote the development of complex *B. subtilis* biofilms on LB medium (Figs 1 and S1, available in the online Supplementary Material, and below).

Using the chemically defined MSgg medium, we observed a marked difference between the colonies developed by all 168 variants and the non-domesticated prototroph; namely, 3610 developed large (18–20 mm), opaque colonies with wrinkles, while all 168 variants developed smaller (5–8 mm) colonies with smooth, bright surfaces on the periphery that show small or no wrinkles (Figs 1 and S1). The opacity in

Table 2. PCR primers used in this study

Primer	Sequence (5′→3′)	Target locus
oTB110	CGAACTGCCGGACAAATC	*epsC*
oTB111	ACGGGCTCTCCCATATC	*epsC*
oTB130	GGTTATGGCTTTTCAGGATCAAAAC	*swrA*
oTB131	TCTATCAAATATTAAATGGCTTGGA TAT	*swrA*
oTB132	CTGTCGTTTCTTTAATATC	*degQ*
oTB133	ACCAGGGATAACGATATCTC	*degQ*
oTB134	GGTGTCAAGCTGTTGATGAG	*sfp*
oTB135	AAGCATCTCCGCCTGTACAC	*sfp*

the wrinkles of a complex colony is suggested to be associated with increased sporulation as the biofilm matures (Arabolaza *et al.*, 2003; Gonzalez-Pastor *et al.*, 2003). These phenotypes are in line with previous reports that define the domesticated 168 strain as a non-biofilm former when grown on MSgg medium (Branda *et al.*, 2001; McLoon *et al.*, 2011). However, the appearance of the biofilms changed drastically when grown on complex medium. On 2×SG, 3610 showed large colonies with increased architectural complexity, i.e. its colonies had larger and seemingly taller wrinkles with opaque white summits, while leaving a clear flat and smooth area in the centre of the colony. On this medium, the 168 variants formed colonies almost as large as those developed by 3610 (15–20 mm), and their topography showed great diversity. 168 P2 and 168 Je, for example, formed wrinkled opaque colonies resembling those formed by 3610 on MSgg, while 168 Gö and 168 NC showed a uniformly rugose, bright surface. On the other hand, JH642 and 168 Bo colonies remained flat with a smooth surface, although they were also larger than those developed on MSgg (Figs 1 and S1). The biofilm colonies grown on LB medium with additional manganese and carbon sources (glycerol and glucose) showed an improvement in the development of wrinkles. 3610 showed an increased formation of wrinkles accompanied by a slightly smaller colony size (15–17 mm), while most 168 variants produced large colonies that even surpassed those of 3610, especially when the medium was supplemented with glucose. On LB-Glu medium, the 168 variants developed opaque colonies that appeared indistinguishable from those of 3610 on MSgg, which suggests that abundance of glucose might be sufficient to overcome the deficiencies observed while developing on MSgg. Strikingly, this is not the case for glycerol, which is the carbon source normally available in MSgg. The colonies developed on LB-Gly, although larger than those on MSgg, still showed reduced complexity with brighter surfaces, as shown before for stock 168 Je (Mhatre *et al.*, 2016).

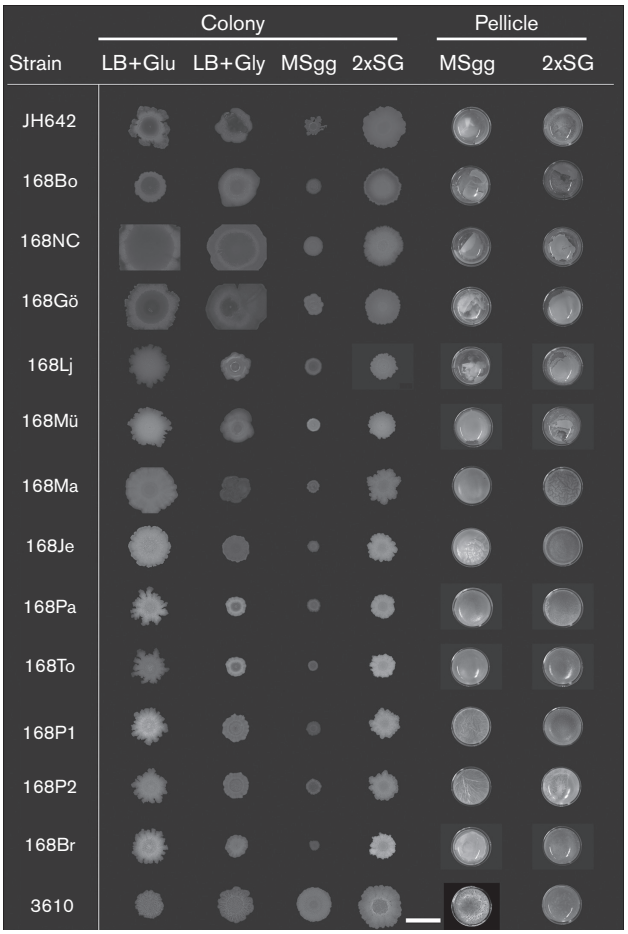

Fig. 1. Comparison of complex colonies and pellicles of *B. subtilis* strain 3610 and 168 variants. Strains were grown on different media and imaged after 72 h incubation, arranged by increasing colony wrinkleability on 2×SG medium. The scale bar shown at the bottom represents 20 mm. Strain abbreviations are described in Table 1.

We tested the development of pellicle biofilms by all 168 variants and 3610 using common biofilm media 2×SG and MSgg after 72 h (Figs 1 and S1). MSgg promotes the formation of densely wrinkled pellicles by 3610, while most 168 variants form thin and flimsy pellicles (e.g. 168 Ma, Pa and To). The most fragile of these pellicles even collapse and sink to the bottom of the well (e.g. 168 Bo, NC, Lj, Gö and JH642). Notable exceptions are the pellicles developed by 168 P1 and P2 strains, which develop thick, wrinkled pellicles similar to those of 3610. Importantly, 2×SG medium promotes the appearance of dense floating biofilm in most 168 variants, except in those that form fragile or collapsed pellicles in MSgg (i.e. 168 Mü, Lj, Gö, NC, Bo and JH642) (Figs 1 and S1). In sum, these experiments suggest that certain variants of *B. subtilis* 168 do develop complex structures on biofilm-promoting, nutrient-rich medium.

Lack of wrinkle formation of complex colony biofilms does not depend exclusively on expression of *epsA-O* and *tapA-sipW-tasA* operons

Biofilm formation by *B. subtilis* has been associated with the development of architecturally complex communities. In this regard, the most recognizable visual phenotype is the development of wrinkles or folds, in both colonies and pellicles (Branda *et al.*, 2001; Kobayashi, 2007). As the production of EPS is closely associated with biofilm development in diverse species (Flemming & Wingender, 2010), we investigated whether the relative expression of the *epsA-O* operon correlates with the appearance of architecturally complex communities. Specifically, we expected that the expression levels from a P_{eps}-GFP reporter fusion would be higher in those strains and under conditions that efficiently develop opaque wrinkles, as compared to those that remain flat and featureless.

To this end, we monitored the levels of green fluorescence during the development of complex colonies of 168 variants

on 2×SG. We selected this medium because the biofilm structures showed a wide range of complexity from the highly wrinkled 3610 reference strain towards the flat and featureless JH642. Surprisingly, we did not observe a correlation between the measured fluorescence levels and the appearance of complex structures in the colonies (Figs 2 and S2). The expression levels of the reporter fusion increased in all 168 variants over time, especially after the onset of stationary phase when colony size extension lessened (around 24 h). However, differences in fluorescence expression appeared without regard to colony wrinkleability. 3610, for example, developed typically complex colonies while maintaining low fluorescence throughout colony development. An inverse correlation was not evident either; JH642 displayed flat, featureless colonies but its fluorescence levels were inferior to those shown by 168 Ma and 168 Br. This result suggests that the expression of the *epsA-O* operon is not directly related to the development of wrinkles during complex colony biofilm formation.

To further test the involvement of other extracellular matrix components over the formation of wrinkles, we measured the expression levels of a P_{tapA}-GFP reporter fusion in the 168 variants. The *tapA-sipW-tasA* operon encodes the protein component of *B. subtilis* biofilms (Branda *et al.*, 2006). *B. subtilis* strains that lack both the *epsA-O* and *tapA-sipW-tasA* operons are unable to form biofilms (Branda *et al.*, 2006; Chu *et al.*, 2006; Romero *et al.*, 2011). We monitored the expression levels of a P_{tapA}-GFP reporter fusion during the development of complex colonies of 168 variants. As in the case of the *epsA-O* operon, 3610 developed a complex wrinkled colony while showing the lowest level of reporter fusion expression, while all 168 variants showed higher fluorescence levels without a clear correlation to wrinkle formation or colony opacity (Figs 3 and S3).

Taken together, these results indicate that the relative expression of genes coding for the EPS and TasA protein matrix components does not directly correlate with the formation of wrinkles in complex colony biofilms of *B. subtilis*. Importantly, it is worth noting that, in both reporter strains, the expression of the corresponding reporter fusion was lowest in the undomesticated 3610 strain.

Differential biofilm formation on roots of *A. thaliana* by diverse 168 stocks

B. subtilis is a soil bacterium known for its ability to colonize plant roots via biofilm development (Beauregard *et al.*, 2013; Chen *et al.*, 2013). We tested whether our previous observations on colony and pellicle robustness would hold true for a root colonization assay, which is a more natural biofilm development model than colonies on agar plates. We examined the colonization of *A. thaliana* roots after 24 h incubation with selected 168 stocks. The stocks used are representative of the diverse colony morphologies previously observed, and were labelled with a $P_{hyperspank}$-GFP reporter fusion in order to detect the bacterial cells using fluorescence microscopy analysis. We observed that the ability to colonize *A. thaliana* roots differs greatly among the 168 stocks tested. Importantly, there is a correlation between a stock's ability to form architecturally complex colonies and root colonization by biofilm development. The non-domesticated isolate 3610 readily colonized the roots over 24 h by developing a large, multi-layered biofilm (Fig. 4a). In contrast, stocks 168

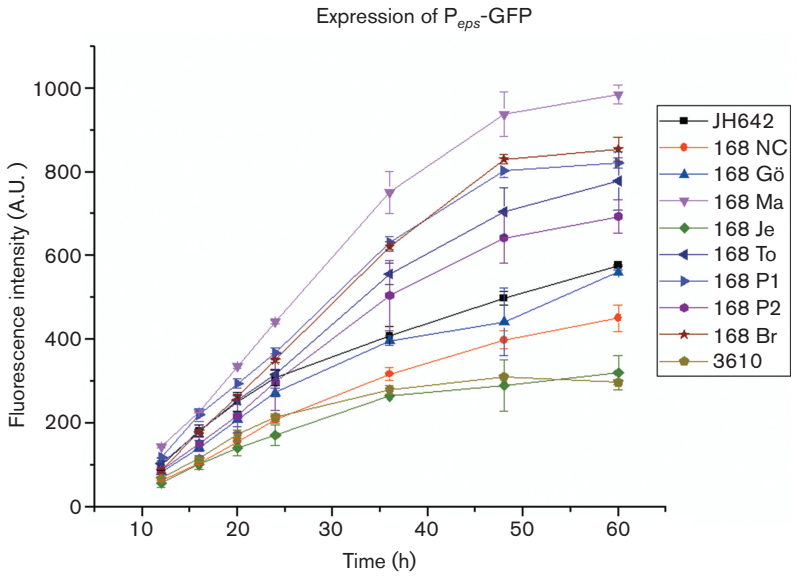

Fig. 2. Fluorescence expression profiles of colonies of *B. subtilis* strain 3610 and 168 variants carrying a transcriptional P_{eps}-GFP fusion. Strains were grown on 2×SG medium and fluorescence was determined at regular intervals as described in Methods. Data points represent the average of three independent colonies. Error bars represent SD. Strain abbreviations are described in Table 1.

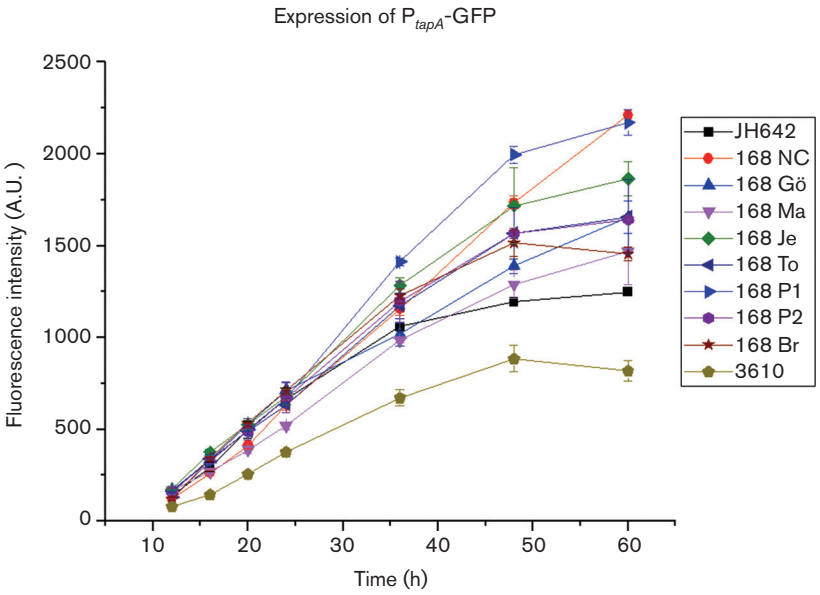

Fig. 3. Fluorescence expression profiles of colonies of *B. subtilis* strain 3610 and 168 variants carrying a transcriptional P_{tapA}-GFP. Strains were grown on 2×SG medium and fluorescence was determined at regular intervals as described in Methods. Data points represent the average of three independent colonies. Error bars represent SD. Strain abbreviations are described in Table 1.

Bo, Gö and Lj were barely present on the root surface, forming small, monolayered attachments (Fig. 4b–d). These stocks are all poor biofilm formers on agar plates. On the other hand, stocks 168 Je and P1 colonized the root surface in a similar fashion as 3610, by forming large biofilms with multiple cell layers (Fig. 4e, f).

To quantitatively strengthen our observations, we estimated the attached bacteria per area of the root surface by measuring the fluorescent intensities originating from the bacterial cells. Using this approach, we corroborated that the average fluorescence intensity per root area was significantly higher in those roots colonized by strain 3610 or stocks 168 Je and P1 as compared to roots colonized by stocks 168 Bo, Gö and Lj (Fig. 4g).

These experiments directly correlate pellicle and colony wrinkleability of *B. subtilis* 168 with the ability to attach and develop biofilm on the plant root surface. Additionally, this also suggests that the biofilm-proficient variants of 168 could be exploited to the study of biofilms in ecological settings.

B. subtilis 168 stocks with a point mutation in *epsC* are poor biofilm formers

Previously, it was reported that a single nucleotide mutation (C to T) at base pair 827 of the *epsC* gene of domesticated *B. subtilis* variants was partially responsible for deficiencies in biofilm development (McLoon *et al.*, 2011). This mutation is responsible for a change from alanine codon 276 (GCG) to a valine codon (GTG), which possibly impairs EPS production. We sequenced a fragment of the *epsC* gene from all the 168 stocks studied in order to investigate whether a consistent relationship exists between the presence of this mutation and deficiencies in biofilm development. We found that all 168 stocks that develop large and flat colonies on 2×SG agar show the C-to-T base substitution in *epsC* (Fig. 5). Among these stocks are 168 Bo, Gö and Lj, which show feeble root colonization. Conversely, stocks that develop architecturally complex colonies on rich media and show efficient root colonization possess the wild-type allele of *epsC* (Fig. 5). The only exception to this trend is 168 Pa, which has the C-to-T mutation but develops architecturally complex colonies on rich media and robust pellicles. 168 Pa was obtained from a 168 parental strain transformed with genomic DNA to repair the tryptophan auxotrophy (Table 1), and *epsC* may have reverted to its wild-type allele during this process while leaving other loci mutated similar to the 168 strains that develop complex wrinkles.

Additionally, we sequenced the relevant fragments of *swrA*, *degQ* and *sfp* to further investigate previously reported gene defects that may be responsible for biofilm formation deficiencies (McLoon *et al.*, 2011). Similar to previous observation (Kovács & Kuipers, 2011), all 168 variants studied and the JH642 strain were found to contain the frameshift (*swrA* or *sfp*) or point (*degQ*) mutations as compared to the corresponding wild-type alleles in 3610 (data not shown); it is thus likely that other loci are different among the various 168 stocks. These results confirm that minimal genetic differences in biofilm-related genes exist among diverse 168 stocks and can lead to drastic phenotypical differences.

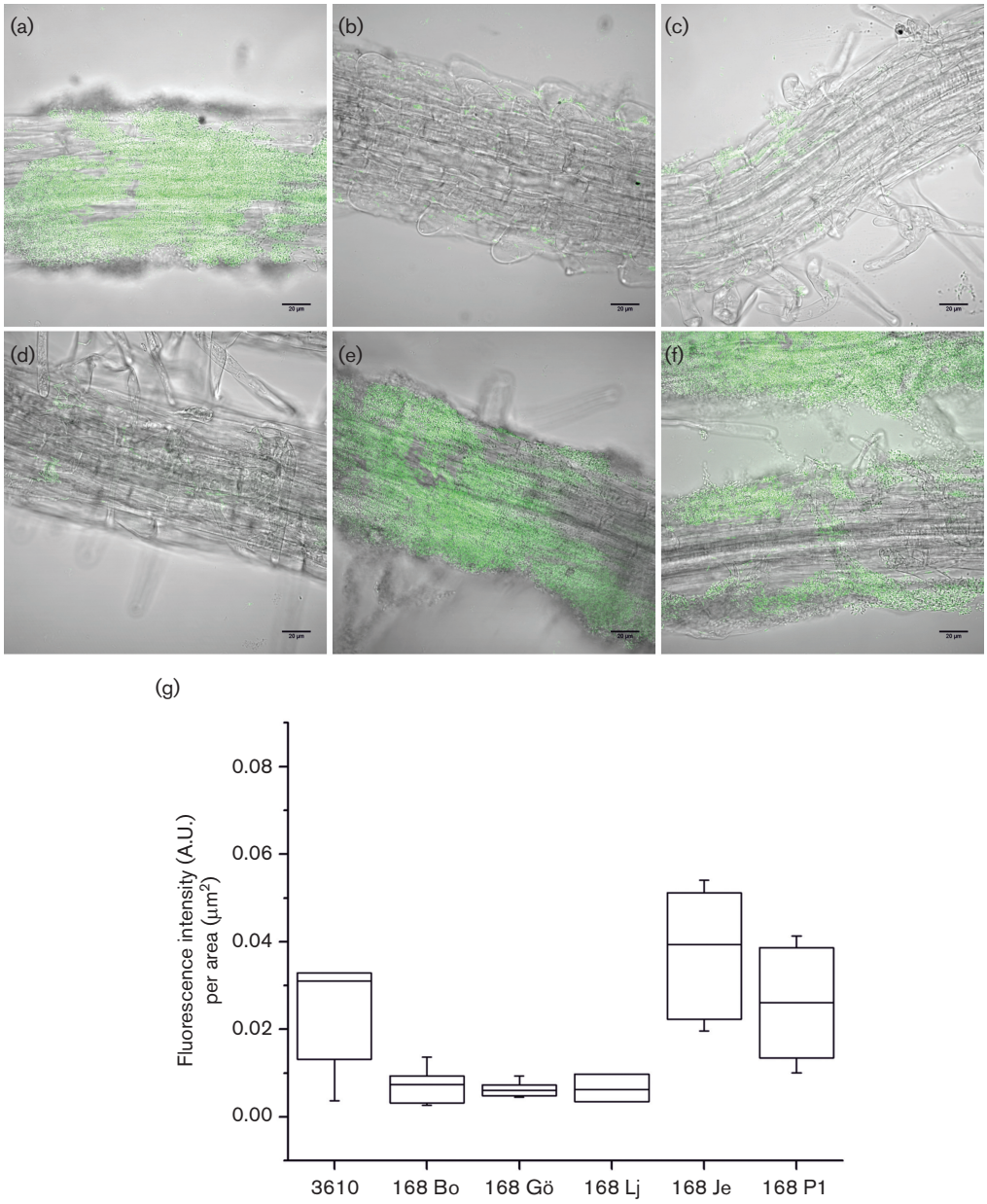

Fig. 4. Colonization of *A. thaliana* roots by selected *B. subtilis* strains. Bacterial cells harbouring a $P_{hyperspank}$-GFP fusion were visualized using fluorescence (false-coloured green) attached to 10- to 12-day-old seedlings of *A. thaliana*. Images are representative of at least six independent roots. The colonization of the plant root surface by *B. subtilis* strains 3610 (a), 168 Bo (b), 168 Gö (c), 168 Lj (d), 168 Je (e) and 168 P1 (f) was quantified as described in Methods and the fluorescent area covered is presented using box plots (g) from at least three scanned areas of three independent roots. Strain abbreviations are described in Table 1.

DISCUSSION

Despite *B. subtilis* being one of the most thoroughly studied bacteria, the process by which it develops its characteristic biofilms is still not completely understood. This may be due to the fact that previous studies focused mainly on the biotechnological potential and metabolic aspects of this organism (Buescher *et al.*, 2012; Nicolas *et al.*, 2012; Öztürk *et al.*, 2016), while its development as a bacterial population has not enjoyed intense research interest until more recently. Detailed investigations on *B. subtilis* interaction with other bacterial and fungal species have been described only recently (Bajaj *et al.*, 2014; Benoit *et al.*, 2015; Powers *et al.*, 2015; Shank *et al.*, 2011; Stanley *et al.*, 2014; Vargas-Bautista *et al.*, 2014). The availability of diverse strains of *B. subtilis* has also hindered biofilm formation research, leading to

Fig. 5. Allelic variation of the *epsC* gene in *B. subtilis* stocks. Alignment of re-sequenced *epsC* gene between base pairs 817 and 837 in all studied *B. subtilis* strains and variants; coded amino acids are indicated above the triplet sequences. The nucleotide at position 827 denoted by a black box for those sequences that present the mutated C-to-T allele. The sequences are arranged by the corresponding phenotype of increasing colony wrinkleability on 2×SG medium. Strain abbreviations are described in Table 1.

contrasting observations about this phenomenon. In addition, other phenotypic features, including flagellum-dependent and -independent surface spreading, called swarming and sliding, respectively, are influenced by the strain and conditions applied (Grau *et al.*, 2015; Kearns & Losick, 2003; Patrick & Kearns, 2009). Spurred by the reported differences among variants of *B. subtilis* 168 strain used in different research laboratories, we present here a thorough comparison of the biofilms developed by various stocks and compared to those of strain 3610. We note that complex, rich media, especially those containing abundant glucose as a carbon source (2×SG and LB-Glu), enable most 168 variants to form large structured colonies. This is strikingly different from the results obtained with MSgg, a chemically defined medium commonly used for biofilm development research, where all 168 variants were unable to develop architecturally complex colonies. Interestingly, carbon-enriched LB medium shows similar observations: the addition of glucose improves the biofilm development of most 168 variants, while glycerol is unable to do so. Additionally, we observed that the same 168 variants that form robust pellicles and complex colonies are able to efficiently colonize *A. thaliana* roots by developing biofilms over the root surface. Interestingly, the medium used in this assay (MSNg) utilizes glycerol as carbon source. The presence of plant exudates may be responsible for promoting efficient biofilm formation in this medium despite the lack of glucose (Beauregard *et al.*, 2013; Castiblanco & Sundin, 2016). Furthermore, all 168 variants that consistently show poor biofilm formation have the same base-pair substitution in the *epsC* gene. This mutation has previously been suggested to be responsible for decreased production of EPS and impaired biofilm formation in 168 variants (McLoon *et al.*, 2011).

The development of wrinkles in *B. subtilis* biofilms is perhaps the most recognizable characteristic of this bacterium. However, the process by which these structures are formed is complex. Localized cell death was shown to determine the location of wrinkle formation (Asally *et al.*, 2012). The channels formed below the wrinkles facilitate liquid flow toward the middle of *B. subtilis* colony biofilms, possibly facilitating nutrient and oxygen transport (Wilking *et al.*, 2013). Our experiments did not show a direct correlation between the magnitude of *epsA-O* and *tapA-sipW-tasA* expression and the formation of said wrinkles. Moreover, strain 3610 showed the lowest expression of the reporter fusion used, with no sign of expression peaks during early biofilm development, as would have perhaps been expected for an efficient biofilm former strain. It is plausible that the expression levels of *epsA-O* and *tapA-sipW-tasA* operons observed in 3610 are sufficient to allow complex colony development, while other genetic factors account for the observed differences in wrinkle formation. In such case, a feedback mechanism might exist that is responsible for increased expression of these reporter fusions in stocks that have reduced wrinkle development. Previously, it was reported that activation of sporulation in colony biofilms of 3610 is delayed in strains lacking EPS production (Aguilar *et al.*, 2010). In such case, the variants with a mutated *epsC* gene would have been expected to have the highest expression levels from P_{eps}-GFP, as they have impaired production of EPS. However, these variants showed only medium expression levels of the reporter fusions, with some of the variants with wild-type alleles of *epsC* showing the highest expression levels of the reporter fusions.

To conclude, the development of biofilms by *B. subtilis* is markedly influenced by available nutrients, especially the carbon source. Due to the variation present in strain 168, we recommend that researchers determine the origin of the particular variant used in their studies. Although more research is necessary to solve the intricacies of these bacterial communities, researchers have to consider the metabolic needs of their laboratory strains before dismissing them as research models.

ACKNOWLEDGEMENTS

We thank Romain Briandet (INRA Jouy-en-Josas, France), Cinzia Calvio (University of Pavia, Italy), Roberto Grau (University of Rosario, Argentina), Elisabeth Härtig (Technische Universität Braunschweig, Germany), Ines Mandić-Mulec (University of Ljubljana, Slovenia), Thorsten Mascher (Technische Universität Dresden, Germany), Mitsuo Ogura (Tokai University, Japan), Jörg Stülke (Georg-August-Universität Göttingen, Germany), Diego Romero (University of Málaga, Spain) and Jan-Willem Veening (University of Groningen, The Netherlands) for kindly providing the various 168 strains, and Nicola Stanley-Wall (University of Dundee, UK) for strains NRS2243 and NRS2394.

The laboratory of Á. T. K. was supported by a Marie Skłodowska Curie career integration grant (PheHetBacBiofilm) and grants KO4741/2-1 and KO4741/3-1 from the Deutsche Forschungsgemeinschaft. R. G.-M. was supported by Consejo Nacional de Ciencia y

Tecnología-German Academic Exchange Service. E.M. was supported though a Jena School for Microbial Communications fellowship. The LSCM780 microscope was financed by a grant from Thüringer Ministerium für Bildung, Wissenschaft und Kultur (project B11024-715).

REFERENCES

Aguilar, C., Vlamakis, H., Guzman, A., Losick, R. & Kolter, R. (2010). KinD is a checkpoint protein linking spore formation to extracellular-matrix production in *Bacillus subtilis* biofilms. *MBio* **1**, e00035-10.

Arabolaza, A. L., Nakamura, A., Pedrido, M. E., Martelotto, L., Orsaria, L. & Grau, R. R. (2003). Characterization of a novel inhibitory feedback of the anti-anti-sigma SpoIIAA on SpoOA activation during development in *Bacillus subtilis*. *Mol Microbiol* **47**, 1251–1263.

Asally, M., Kittisopikul, M., Rué, P., Du, Y., Hu, Z., Çağatay, T., Robinson, A. B., Lu, H., Garcia-Ojalvo, J. & Süel, G. M. (2012). Localized cell death focuses mechanical forces during 3D patterning in a biofilm. *Proc Natl Acad Sci U S A* **109**, 18891–18896.

Bais, H. P., Fall, R. & Vivanco, J. M. (2004). Biocontrol of *Bacillus subtilis* against infection of arabidopsis roots by *Pseudomonas syringae* is facilitated by biofilm formation and surfactin production. *Plant Physiol* **134**, 307–319.

Bajaj, I., Veiga, T., van Dissel, D., Pronk, J. T. & Daran, J. M. (2014). Functional characterization of a *Penicillium chrysogenum* mutanase gene induced upon co-cultivation with *Bacillus subtilis*. *BMC Microbiol* **14,** 114.

Barbe, V., Cruveiller, S., Kunst, F., Lenoble, P., Meurice, G., Sekowska, A., Vallenet, D., Wang, T., Moszer, I. & other authors (2009). From a consortium sequence to a unified sequence: the *Bacillus subtilis* 168 reference genome a decade later. *Microbiology* **155**, 1758–1775.

Beauregard, P. B., Chai, Y., Vlamakis, H., Losick, R. & Kolter, R. (2013). *Bacillus subtilis* biofilm induction by plant polysaccharides. *Proc Natl Acad Sci U S A* **110**, E1621–E1630.

Benoit, I., van den Esker, M. H., Patyshakuliyeva, A., Mattern, D. J., Blei, F., Zhou, M., Dijksterhuis, J., Brakhage, A. A., Kuipers, O. P. & other authors (2015). *Bacillus subtilis* attachment to *Aspergillus niger* hyphae results in mutually altered metabolism. *Environ Microbiol* **17**, 2099–2113.

Bjarnsholt, T., Alhede, M., Alhede, M., Eickhardt-Sørensen, S. R., Moser, C., Kühl, M., Jensen, P. Ø. & Høiby, N. (2013). The *in vivo* biofilm. *Trends Microbiol* **21**, 466–474.

Branda, S. S., González-Pastor, J. E., Ben-Yehuda, S., Losick, R. & Kolter, R. (2001). Fruiting body formation by *Bacillus subtilis*. *Proc Natl Acad Sci U S A* **98**, 11621–11626.

Branda, S. S., González-pastor, J. E., Ehrlich, S. D., Losick, R., Gonza, E. & Dervyn, E. (2004). Genes involved in formation of structured multicellular communities by *Bacillus subtilis*. *J Bacteriol* **186**, 3970–3979.

Branda, S. S., Chu, F., Kearns, D. B., Losick, R. & Kolter, R. (2006). A major protein component of the *Bacillus subtilis* biofilm matrix. *Mol Microbiol* **59**, 1229–1238.

Buescher, J. M., Liebermeister, W., Jules, M., Uhr, M., Muntel, J., Botella, E., Hessling, B., Kleijn, R. J., Le Chat, L. & other authors (2012). Global network reorganization during dynamic adaptations of *Bacillus subtilis* metabolism. *Science* **335**, 1099–1103.

Burkholder, P. & Giles, N. H. (1947). Induced biochemical mutations in *Bacillus subtilis*. *Am J Bot* **34**, 345–348.

Cairns, L. S., Hobley, L. & Stanley-Wall, N. R. (2014). Biofilm formation by *Bacillus subtilis*: new insights into regulatory strategies and assembly mechanisms. *Mol Microbiol* **93**, 587–598.

Castiblanco, L. F. & Sundin, G. W. (2016). New insights on molecular regulation of biofilm formation in plant-associated bacteria. *J Integr Plant Biol* **58**, 362–372.

Chai, Y., Beauregard, P. B., Vlamakis, H., Losick, R. & Kolter, R. (2012). Galactose metabolism plays a crucial role in biofilm formation by *Bacillus subtilis*. *MBio* **3**, e00184-12.

Chen, Y., Yan, F., Chai, Y., Liu, H., Kolter, R., Losick, R. & Guo, J. H. (2013). Biocontrol of tomato wilt disease by *Bacillus subtilis* isolates from natural environments depends on conserved genes mediating biofilm formation. *Environ Microbiol* **15**, 848–864.

Chu, F., Kearns, D. B., Branda, S. S., Kolter, R. & Losick, R. (2006). Targets of the master regulator of biofilm formation in *Bacillus subtilis*. *Mol Microbiol* **59**, 1216–1228.

Earl, A. M., Losick, R. & Kolter, R. (2008). Ecology and genomics of *Bacillus subtilis*. *Trends Microbiol* **16**, 269–275.

Flemming, H.-C. & Wingender, J. (2010). The biofilm matrix. *Nat Rev Microbiol* **8**, 623–633.

Gonzalez-Pastor, J. E., Hobbs, E. C. & Losick, R. (2003). Cannibalism by sporulating bacteria. *Science* **301**, 510–513.

Grau, R. R., de Oña, P., Kunert, M., Leñini, C., Gallegos-Monterrosa, R., Mhatre, E., Vileta, D., Donato, V., Hölscher, T. & other authors (2015). A duo of potassium-responsive histidine kinases govern the multicellular destiny of *Bacillus subtilis*. *MBio* **6**, e00581-15.

Harwood, C. R. & Cutting, S. M. (1990). *Molecular Biological Methods for Bacillus*. Chichester, England: John Wiley & Sons Ltd.

Jones, S. E., Paynich, M. L., Kearns, D. B. & Knight, K. L. (2014). Protection from intestinal inflammation by bacterial exopolysaccharides. *J Immunol* **192**, 4813–4820.

Kearns, D. B. & Losick, R. (2003). Swarming motility in undomesticated *Bacillus subtilis*. *Mol Microbiol* **49**, 581–590.

Kearns, D. B., Chu, F., Branda, S. S., Kolter, R. & Losick, R. (2005). A master regulator for biofilm formation by *Bacillus subtilis*. *Mol Microbiol* **55**, 739–749.

Kobayashi, K. (2007). *Bacillus subtilis* pellicle formation proceeds through genetically defined morphological changes. *J Bacteriol* **189**, 4920–4931.

Kohlstedt, M., Sappa, P. K., Meyer, H., Maaß, S., Zaprasis, A., Hoffmann, T., Becker, J., Steil, L., Hecker, M. & other authors (2014). Adaptation of *Bacillus subtilis* carbon core metabolism to simultaneous nutrient limitation and osmotic challenge: a multi-omics perspective. *Environ Microbiol* **16**, 1898–1917.

Konkol, M. A., Blair, K. M. & Kearns, D. B. (2013). Plasmid-encoded ComI inhibits competence in the ancestral 3610 strain of *Bacillus subtilis*. *J Bacteriol* **195**, 4085–4093.

Kovács, A. T. & Kuipers, O. P. (2011). Rok regulates yuaB expression during architecturally complex colony development of *Bacillus subtilis* 168. *J Bacteriol* **193**, 998–1002.

Kunst, F. & Rapoport, G. (1995). Salt stress is an environmental signal affecting degradative enzyme synthesis in *Bacillus subtilis*. *J Bacteriol* **177**, 2403–2407.

Kunst, F., Ogasawara, N., Moszer, I., Albertini, A. M., Alloni, G., Azevedo, V., Bertero, M. G., Bessières, P., Bolotin, A. & other authors (1997). The complete genome sequence of the Gram-positive bacterium *Bacillus subtilis*. *Nature* **390**, 249–256.

McLoon, A. L., Guttenplan, S. B., Kearns, D. B., Kolter, R. & Losick, R. (2011). Tracing the domestication of a biofilm-forming bacterium. *J Bacteriol* **193**, 2027–2034.

Meyer, H., Weidmann, H., Mäder, U., Hecker, M., Völker, U. & Lalk, M. (2014). A time resolved metabolomics study: the influence of different carbon sources during growth and starvation of *Bacillus subtilis*. *Mol Biosyst* **10**, 1812–1823.

Mhatre, E., Monterrosa, R. G. & Kovács, A. T. (2014). From environmental signals to regulators: modulation of biofilm development in Gram-positive bacteria. *J Basic Microbiol* **54**, 616–632.

Mhatre, E., Troszok, A., Gallegos-Monterrosa, R., Lindstädt, S., Hölscher, T., Kuipers, O. P. & Kovács, Á. T. (2016). The impact of manganese on biofilm development of *Bacillus subtilis*. *Microbiology* **162**, 1468–1478.

Mielich-Süss, B. & Lopez, D. (2015). Molecular mechanisms involved in *Bacillus subtilis* biofilm formation. *Environ Microbiol* **17**, 555–565.

Murray, E. J., Strauch, M. A. & Stanley-Wall, N. R. (2009). SigmaX is involved in controlling *Bacillus subtilis* biofilm architecture through the AbrB homologue Abh. *J Bacteriol* **191**, 6822–6832.

Nicolas, P., Mäder, U., Dervyn, E., Rochat, T., Leduc, A., Pigeonneau, N., Bidnenko, E., Marchadier, E., Hoebeke, M. & other authors (2012). Condition-dependent transcriptome reveals high-level regulatory architecture in *Bacillus subtilis*. *Science* **335**, 1103–1106.

Oslizlo, A., Stefanic, P., Vatovec, S., Beigot Glaser, S., Rupnik, M. & Mandic-Mulec, I. (2015). Exploring ComQXPA quorum-sensing diversity and biocontrol potential of *Bacillus* spp. isolates from tomato rhizoplane. *Microb Biotechnol* **8**, 527–540.

Öztürk, S., Çalık, P. & Özdamar, T. H. (2016). Fed-batch biomolecule production by *Bacillus subtilis*: a state of the art review. *Trends Biotechnol* **34**, 329–345.

Patrick, J. E. & Kearns, D. B. (2009). Laboratory strains of *Bacillus subtilis* do not exhibit swarming motility. *J Bacteriol* **191**, 7129–7133.

Pollak, S., Omer Bendori, S. & Eldar, A. (2015). A complex path for domestication of *B. subtilis* sociality. *Curr Genet* **61**, 493–496.

Powers, M. J., Sanabria-Valentín, E., Bowers, A. A. & Shank, E. A. (2015). Inhibition of cell differentiation in *Bacillus subtilis* by *Pseudomonas protegens*. *J Bacteriol* **197**, 2129–2138.

Romero, D. (2013). Bacterial determinants of the social behavior of *Bacillus subtilis*. *Res Microbiol* **164**, 788–798.

Romero, D., Vlamakis, H., Losick, R. & Kolter, R. (2011). An accessory protein required for anchoring and assembly of amyloid fibres in *B. subtilis* biofilms. *Mol Microbiol* **80**, 1155–1168.

Roux, D., Cywes-Bentley, C., Zhang, Y. F., Pons, S., Konkol, M., Kearns, D. B., Little, D. J., Howell, P. L., Skurnik, D. & Pier, G. B. (2015). Identification of poly-*N*-acetylglucosamine as a major polysaccharide component of the *Bacillus subtilis* biofilm matrix. *J Biol Chem* **290**, 19261–19272.

Seccareccia, I., Kovács, Á. T., Gallegos-Monterrosa, R. & Nett, M. (2016). Unraveling the predator-prey relationship of *Cupriavidus necator* and *Bacillus subtilis*. *Microbiol Res* **192**, 231–238.

Shank, E. A. & Kolter, R. (2011). Extracellular signaling and multicellularity in *Bacillus subtilis*. *Curr Opin Microbiol* **14**, 741–747.

Shank, E. A., Klepac-Ceraj, V., Collado-Torres, L., Powers, G. E., Losick, R. & Kolter, R. (2011). Interspecies interactions that result in *Bacillus subtilis* forming biofilms are mediated mainly by members of its own genus. *Proc Natl Acad Sci U S A* **108**, E1236–E1243.

Stanley, C. E., Stöckli, M., van Swaay, D., Sabotič, J., Kallio, P. T., Künzler, M., DeMello, A. J. & Aebi, M. (2014). Probing bacterial–fungal interactions at the single cell level. *Integr Biol* **6**, 935–945.

Valderrama, W. B. & Cutter, C. N. (2013). An ecological perspective of *Listeria monocytogenes* biofilms in food processing facilities. *Crit Rev Food Sci Nutr* **53**, 801–817.

van Gestel, J., Weissing, F. J., Kuipers, O. P. & Kovács, A. T. (2014). Density of founder cells affects spatial pattern formation and cooperation in *Bacillus subtilis* biofilms. *ISME J* **8**, 2069–2079.

Vargas-Bautista, C., Rahlwes, K. & Straight, P. (2014). Bacterial competition reveals differential regulation of the *pks* genes by *Bacillus subtilis*. *J Bacteriol* **196**, 717–728.

Vlamakis, H., Chai, Y., Beauregard, P., Losick, R. & Kolter, R. (2013). Sticking together: building a biofilm the *Bacillus subtilis* way. *Nat Rev Microbiol* **11**, 157–168.

Wilking, J. N., Zaburdaev, V., De Volder, M., Losick, R., Brenner, M. P. & Weitz, D. A. (2013). Liquid transport facilitated by channels in *Bacillus subtilis* biofilms. *Proc Natl Acad Sci U S A* **110**, 848–852.

Zeigler, D. R., Prágai, Z., Rodriguez, S., Chevreux, B., Muffler, A., Albert, T., Bai, R., Wyss, M. & Perkins, J. B. (2008). The origins of 168, W23, and other *Bacillus subtilis* legacy strains. *J Bacteriol* **190**, 6983–6995.

Edited by: T. Msadek and Jö. Stülke